Cylindrical Pores Responding to Two Different Stimuli via Surface-Initiated Atom Transfer Radical Polymerization for Synthesis of Grafted Diblock Copolymers

Alexander Friebe and Mathias Ulbricht*[,†,†,‡]

Lehrstuhl für Technische Chemie II, Universität Duisburg-Essen, 45141 Essen, Germany, and CeNIDE−Centre for Nanointegration Duisburg-Essen, 47057 Duisburg, Germany

Received September 26, 2008; Revised Manuscript Received December 19, 2008

ABSTRACT: Functional polymeric materials with cylindrical pores where effective pore size can be significantly and reversibly manipulated by combination of two different stimuli, here combinations of pH and temperature, have been successfully prepared by surface-selective ATRP from the pore surface of track-etched poly(ethylene terephthalate) membranes with pore diameters of 790 and 1900 nm. Initiator immobilization on the poly(ethylene terephthalate) surface in a density of ∼1 group per nm^2 was done via already reported solid phase chemistry. An ATRP system with copper(I) chloride/tris(2-(dimethylamino)ethyl)amine as catalyst and *N*,*N*-dimethylformamid as solvent was established what allows the controlled grafting of poly(*N*-isopropyl acrylamide) and poly(*tert*-butyl acrylate) and of their diblock copolymers in both different sequences. Conditions for hydrolysis of grafted poly(*tert*-butyl acrylate) to poly(acrylic acid) in the poly(ethylene terephthalate) pores without changing the substrate structure had also been established. The well-defined porous polymer substrate allowed to obtain qualitative and quantitative information on the functional layers in dry state (from gravimetry, IR spectroscopy and liquid dewetting permporometry), and—via analysis of membrane permeability—on effective thickness, density and reversible swelling ratio of these grafted layers in wet state. It is remarkable that dry poly(*N*-isopropyl acrylamide) layer thicknesses of several hundred nanometers could be obtained in only 4 h reaction time. All data indicate that grafted poly(*N*-isopropyl acrylamide) and poly(acrylic acid) with a "brush" structure have been achieved; however, the poly(*N*-isopropyl acrylamide) brush layers had a higher density what could be related to the lower reactivity of the functional monomer. The effective layer thickness of the grafted diblock copolymer layers could be reversibly changed in four steps by up to 200 nm via different combinations of pH (between 2 and 7) and temperature (23 and 45 °C).

Introduction

The controlled functionalization of a material's surfaces with "smart", stimuli-responsive polymers which change their properties strongly with small changes of the environmental conditions is of rapidly increasing scientific and technical interest. An important group are surface-functionalized "smart" materials in contact with a liquid, in particular an aqueous phase; their surface properties such as wetting, swelling or flexibility can be "switched" by changes of temperature, pH value, ionic strength, presence of certain ions or molecules, etc.[1,2] The transfer of such functionalizations to surfaces of pores or channels leads to stimuli-responsive, "switchable" membranes[3] or microfluidic systems,[2,4−6] respectively.

In order to "tailor" the surface functionality, the "grafting-from" approach, i.e., a heterogeneous graft copolymerization of functional monomers initiated at the material's surface, has notable advantages because the resulting macromolecular layers can be prepared in a wide range with respect to thickness, internal structure and architectures (e.g., "brush" vs "mushroom" or cross-linked) and functional groups; numerous interesting and versatile examples have been reported.[7] However, there is still a demand for methods where the grafting density and the grafted chain lengths including low polydispersity can be precisely adjusted or where well-defined architectures such as block copolymers can be synthesized via "grafting-from"; this is especially true for the functionalization within pores or microchannels and with technical polymers as substrate.

Atom transfer radical polymerization (ATRP), typically based on an alkylhalide as initiator and a complexed copper(I)/copper(II) system as catalyst, allows the controlled synthesis of macromolecules from a wide range of monomers under facile reaction conditions. Attractive features of ATRP are low polydispersity and the possibility of reinitiation to synthesize block copolymers, both related to the "living" character of the chain growth reaction. In addition, the options—with highly reactive catalysts—to work at low temperatures and to use a wide range of solvents make ATRP very attractive.[8−10] Consequently, ATRP has also been intensively explored for surface functionalization, first with well-defined planar model surfaces such as self-assembled monolayers on gold or silica,[11−16] and more recently also with polymer films.[17−19] Examples for the controlled functionalization of porous substrates,[20,21] especially porous membranes, via surface-initiated ATRP are still rare. Zhai et al. reported on the preparation of a macroporous membrane from a graft copolymer of 2-(2-bromoisobutyryloxy)-ethyl acrylate (an "inimer" containing an ATRP initiator) on poly(vinylidene fluoride) and the subsequent surface functionalization of the membranes via ATRP.[22] Husson et al. premodified poly(vinylidene fluoride) membranes with poly(glycidyl methacrylate to covalently immobilize the initiator and grafted then poly(2-vinylpyridine) via ATRP.[23] Xu et al. immobilized the ATRP initiator on the surface of nylon membranes and performed ATRP grafting of poly(2-hydroxyethyl methacrylate) and poly(ethylene glycol)monomethacrylate.[24] Yang et al. functionalized macroporous polypropylene membranes, in a first step via UV initiated grafting with a thin film of poly(2-hydroxyethyl methacrylate) in order to covalently couple the ATRP initiator in this layer, in a second step by ATRP of a glycosylated acrylate monomer.[25] Bruening et al. had used

* Corresponding author. Fax: x49-201-183 3147. E-mail: mathias.ulbricht@uni-essen.de.
† Lehrstuhl für Technische Chemie II, Universität Duisburg-Essen.
‡ CeNIDE−Centre for Nanointegration Duisburg-Essen.

10.1021/ma802185d CCC: $40.75
Published on Web 02/04/2009

porous membranes from aluminum oxide after initiator immobilization via silanization for ATRP grafting of poly(2-hydroxyethyl methacrylate); the subsequent derivatization of the side groups of the grafted polymer lead to a high-capacity pseudoaffinity membrane adsorber.[26] A high-capacity ion-exchange membrane adsorber had been obtained via direct initiator immobilization on regenerated cellulose and subsequent ATRP grafting the sodium salt of acrylic acid.[27]

Very frequently studied prototypes for stimuli-responsive polymers are poly(acrylic acid) (PAA), with a transition between collapsed and swollen state upon increasing the pH above the pK_a (~4.5), and poly(*N*-isopropylacrylamide) (PNIPAAm), having a lower critical solution temperature of 32 °C. The latter polymer is of particular interest for "smart" soft materials due to the very pronounced decrease in swelling upon a very small increase in temperature around the lower critical solution temperature.[28] Combinations of different polymers, e.g. PNIPAAm hydrogels with grafted PAA chains, have also been described as example for materials which can reversibly swell/deswell as function of the combination of pH and temperature.[29,30] Dual-responsive surfaces based on random PAA/PNIPAAm copolymers on structured substrates that switch between superhydrophilic and superhydrophobic properties had recently been reported.[31] In another study, block copolymers of PNIPAAm and poly(4-vinylpyridine) with dual-responsive properties were grafted from cellulose.[32] Polymerization of acrylic acid (AA) via ATRP is complicated because of complexation of copper which is an essential component of the catalyst system. Recently, examples for the successful use of the salt of AA in an aqueous system for controlled surface-initiated ATRP have been reported.[27,33] An alternative is the ATRP of *tert*-butyl acrylate (tBA) and subsequent hydrolysis of the side groups to yield the grafted PAA.[11] *N*-Isopropylacrylamide (NIPAAm) is a monomer which is also difficult to control under ATRP conditions. Masci et al. improved the reaction conditions by using either pure *N*,*N*-dimethylformamid (DMF) or mixtures of DMF with water, and they obtained at room temperature in shorter time higher molar masses without loss of control.[34]

In previous work, poly(ethylene terephthalate) track-etched membranes (PET TEM) with uniform cylindrical pores at very narrow size distribution had been established as a versatile tool to investigate various grafting reactions in pores and the effects on material's function.[3,35] It had been demonstrated that under appropriate experimental conditions, effective thicknesses (in the range of a few to several hundred nanometers) of grafted polymer layers on the pore walls could be precisely estimated from membrane permeability data.[36] Using PET TEM with pore diameter of 790 nm as substrate, we had recently reported on the controlled pore surface functionalization via immobilization of a bromoalkyl initiator in varied density on the premodified PET surface, and subsequent surface-initiated ATRP of NIPAAm from a methanol/water system.[37] Shortly after our paper, Alem et al.[38] published a study where PET TEM had also been functionalized under ATRP conditions with PNIPAAm. However, the bromoalkyl initiator had been immobilized directly on the surface of the original membrane, so that the initiator and grafting density had been much lower than in our work. A presumably less controlled polymerization in combination with smaller pore size (330 or even 80 nm), both in comparison with our work, lead to a more uneven functionalization of internal vs outer membrane surface (even plugging of pores by a layer on the outer membrane surface) and less defined response of membrane permeability to temperature changes.

It was the aim of this work to synthesize materials with cylindrical pores where the effective pore size can be significantly and reversibly manipulated by the combination of two different stimuli (Scheme 1). We report on the controlled and relatively fast synthesis of stimuli-responsive functional polymer layers at high density and with high molar mass on the inner pore surface of TEM from the technically relevant polymer PET. We used an ATRP system with DMF or DMF/2-butanone as solvent, what allows the controlled grafting of PNIPAAm and PtBA, and of their block copolymers in both different sequences. With both monomers, tBA and NIPAAm, we investigated the initiation efficiencies either with the bromoalkyl initiator directly on the PET surface or with a first grafted polymer block as macroinitiator. Conditions for the hydrolysis of grafted poly(*tert*-butyl acrylate) (PtBA) to PAA on/in the PET TEM without changing the substrate pore structure had also been established. In contrast to numerous other studies where such homo- or blockcopolymer architectures had been synthesized on planar inorganic substrates, we could use the special properties of the well-defined porous polymer membrane substrate to obtain qualitative and quantitative information on the functional layers in dry state (here mainly from gravimetry, IR spectroscopy and liquid dewetting permporometry), and—via analysis of membrane permeability—on effective thickness, density and reversible swelling ratio of these grafted layer in wet state. To the best of our knowledge, this is the first report on the synthesis of grafted diblock copolymers at high density via controlled "living" polymerization in cylindrical pores, leading to new materials behaving as "microvalves" with four distinctly different barrier dimensions as function of the combination of two different stimuli.

Scheme 1. Combination of Two Stimuli-Responsive Polymers with Low Polydispersity as Grafted Diblock Copolymer Brushes in Cylindrical Pores Leading to Four Different Effective Pore Diameters as a Function of the Combination of the Two Stimuli (Temperature Change, ΔT, around the Lower Critical Solution Temperature of the First Polymer Block/Here: PNIPAAm; pH change, ΔpH, around the pK_a of the Second Polymer Block/Here: PAA)

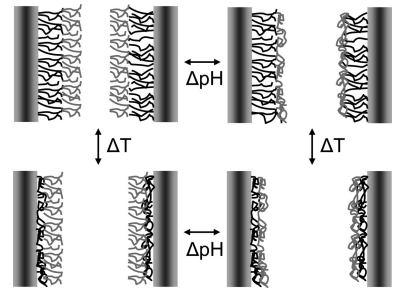

Experimental Section

Materials. PET track-etched membranes Rotrac with a nominal pore diameter of 400 nm (thickness: 23 μm) and 1000 nm (thickness: 22 μm) were from Oxyphen GmbH, Dresden, Germany. Succinic anhydride, 99+%; copper(I) chloride, 99.99%; and copper(II) bromide, 99+% anhydrous and extra pure; were purchased from Acros Organics and used as received. *tert*-Butyl acrylate (tBA), 99% stabilized; was also from Acros and purified by distillation from calcium hydride under argon (purity 5.0) atmosphere at 60 mbar pressure. Methanesulfonic acid, ≥99.5%; and *N*-isopropylacrylamide (NIPAAm), 97%; were obtained from Sigma-Aldrich. NIPPAm was recrystallized twice from n-hexane to remove the inhibitor. Both monomers were stored until use under argon in the dark at 2 °C in a refrigerator. 4-(*N*′,*N*′-Dimethylamino)pyridine, 99.5% pure; thionin acetate, for microscopy; 2-butanone, pure; and *N*,*N*,*N*′,*N*″,*N*″-pentamethyl diethylenetriamine, pure, were from Fluka and also used as received. *N*,*N*-Dimethylformamide (DMF), pure; was from AppliChem and dichloromethane, 99% pure; was from Baker. All other solvents were obtained from VWR-BDH-Prolabo and used as received. Tris(2-(dimethylamino)ethyl)amine (Me_6TREN) was synthesized according to Ciampolini et al.[39]

Syntheses. The membrane samples were all cut into 25 mm diameter disks. The pretreatment, "oxidative hydrolysis" and the two step functionalization including the final immobilization of the α-bromoisobutyryl ATRP-initiator was done as reported in earlier papers.[35−37] Before grafting, the samples were dried for 1 h at 45 °C and weighed using a GENIUS balance (accuracy: ±10 μg) from Sartorius (Germany).

Quantitative Determination of Functional Groups of PET. Carboxyl groups analysis on PET surfaces was performed by reversible binding of the cationic dye thionin acetate according to the method described earlier.[35] The hydroxyl groups were determined as follows: Each sample was immersed in 10 mL of an acetonitrile solution containing 100 mg succinic anhydride and 150 mg 4-(*N*′,*N*′-dimethylamino)pyridine for 3 h at 55 °C. The reaction was carried out in test tubes with 28 mm diameter, closed with a rubber septum to protect the solution against moisture. Thereafter the samples were washed in acetonitrile and subsequently twice in methanol. Then, the reversible binding of thionin acetate was repeated after derivatization of hydroxyl- to carboxyl groups. The difference between both measured surface concentrations before and after conversion represents the amount of hydroxyl groups.

Surface-Initiated ATRP—Synthesis of Single Blocks and Block-Copolymers. The ATRP reactions were carried out in a house made setup of 100 mL 3-neck flasks with septum and gastight screw caps under argon atmosphere. This setup allowed the parallel functionalization of up to eighteen membrane samples (one per flask) using the same reaction mixture and, if intended, different reaction times. The reaction solution was prepared in a 100 mL 4-neck flask with septum. For a typical experiment 12.03 g of NIPAAm (or 15.5 mL of tBA) and 244 μL of Me_6TREN were dissolved in DMF to yield 25 mL solution (=4.25 mol/L monomer). After 45 min degassing with argon, 88 mg of copper(I) chloride was added with strong stirring under a continuous argon stream. The molar ratio in all experiments was [Monomer]:[Me_6TREN]:[copper(I) chloride] = [120]:[1]:[1]. Me_6TREN leads in DMF to partial disproportionation of copper(I) to copper(0) and (II).[40] When a pale (red-brown for NIPAAm, green-gray for tBA) and troubled suspension had been formed, a volume of 6 mL was injected with a 10 mL gastight syringe with silicon plunger (B. Braun Melsungen AG, Melsungen, Germany) through the septum into the flask containing one membrane sample. To stop the polymerization the screw caps were opened, the samples were quickly removed and immersed in 10 mL of a solution of 50 mg copper(II) bromide and 125 μL *N*,*N*,*N*′,*N*′′,*N*′′-pentamethyl diethylenetriamine in degassed DMF to avoid oxygen contact. The washing procedure was as follows: The first solution, 10 mL for each sample, contained 125 μL *N*,*N*,*N*′,*N*′′,*N*′′-pentamethyl diethylenetriamine in DMF to remove copper traces. Subsequently, the samples were washed twice DMF. In the last solution, the samples remained for 45 min. Subsequently, the samples were washed for 1 h in methanol. After drying at 50 °C for 2 h, the samples were weighed again to determine the degree of graft functionalization, which was calculated according to:

$$\mathrm{DG} = \frac{m_{gr} - m_o}{A_{spec}} \quad (1)$$

where m_o is the membrane sample weight after initiator immobilization, m_{gr} is the membrane weight after grafting, and A_{spec} is the specific surface area of the used 25 mm membranes (112.69 cm^2 for PET400 and 35.11 cm^2 for PET1000). Considering the accuracy of the balance, the smallest weight difference what can be measured (±10 μg; cf. above), corresponds to a DG difference of ± 0.1 μg/cm^2 (PET400) and ± 0.3 μg/cm^2 (PET1000) for the sample with a diameter of 25 mm (cf. above). The dry layer thickness, l_{dry}, was calculated from DG assuming a polymer density of 1.1 g/cm^3 and even coverage of the entire surface area.

Hydrolysis of PtBA to PAA. To obtain pH-responsive PAA, the samples grafted with PtBA were treated for 15 min in a 1% solution of methanesulfonic acid in dichloromethane at room temperature. After hydrolysis the samples were washed in DMF to remove residues of methanesulfonic acid and finally for 1 h in methanol. Subsequently the samples were dried for 2 h at 50 °C.

Table 1. Overview on Properties of the Base Poly(ethylene terephthalate) Track-Etched Membranes Used in This Work (Original = As Received; with Initiator = after Oxidative Hydrolysis and Two-Step Immobilization of ATRP Initiator According to Ref 37)

membrane	thickness [μm]	porosity [%]	specific area [cm^2/cm^2]	pore density [cm^{-2}]	pore diameter [nm] original	pore diameter [nm] with initiator
PET400	23	18.3	22.96	37×10^6	760	790 ± 17
PET1000	22	11.7	7.15	4.1×10^6	1809	1914 ± 23

Measurements. Pore size distributions of membranes in dry state were measured by using permporometry ("liquid displacement") with a capillary flow porometer from PMI (New York) as described in detail before.[35,36] The measurements of pure water permeability were performed in a 3 mL Amicon cell (Millipore, MA), and the estimation of membrane pore density for virgin membranes was done as described in our earlier paper.[37] The pore size of the membranes in wet state was then calculated from the permeability data by using the equation of Hagen-Poiseuille:

$$\frac{V}{\Delta t} = \frac{\pi \Delta P r^4}{8 \eta L} \quad (2)$$

where V is the volume of the permeate relating to a single cylindrical membrane pore, Δt is the time interval, ΔP is the trans-membrane pressure, r is the pore radius, η is the viscosity of water, and L is the capillary length, i.e. the membrane thickness. The first result is the effective hydrodynamic pore diameter, d_h (= 2·r). The thickness of the grafted layer on the pore wall, l_h, is calculated as the difference between the pore radius of the initiator-immobilized membrane and the pore radius of the grafted membrane.

Results and Discussion

Characterization of PET Membranes before and after Polymer-Analogous Syntheses. Pore Size Distribution. The methods for solid phase synthesis on the inner and outer surface of the PET TEM had been developed to achieve an adjustable density of initiator groups covering a wide range which will allow a variation of grafting density during ATRP.[37] At the same time, the narrow pore size distribution of the base membrane should be maintained during all steps to the grafted PET pores.

The pore diameter of the PET400 membranes after initiator immobilization was 790 ± 17 nm, slightly higher as compared with the diameter of ∼760 nm of the virgin samples (Table 1). This increase is caused by the oxidative hydrolysis.[37] Membrane pore density and thickness were not influenced by the oxidative hydrolysis. Exactly the same trends were observed for the PET1000 membranes (cf. Table 1).

Measurements via two independent methods, SEM (Figure 1) and permporometry (cf. Supporting Information), show that the isocylindrical pore morphology of the membranes was preserved until the final stage of the functionalization sequence (for ATRP conditions see below). All pore entrances were significantly smaller than for the unmodified membrane, but pore shape was unchanged (cf. Figure 1). Even samples with high DG had still a narrow pore size distribution indicating an even coverage of the entire pore surface (cf. Supporting Information). This preservation of the base pore structure is a precondition to calculate the specific surface area (to convert the DG to dry layer thickness) and the pore radii in wet state from water permeability (to deduce information on effective wet layer thickness).

Functional Group Density on the Surface. The surface of PET contains already a significant density of hydroxyl and carboxyl groups after the process of membrane manufacture by

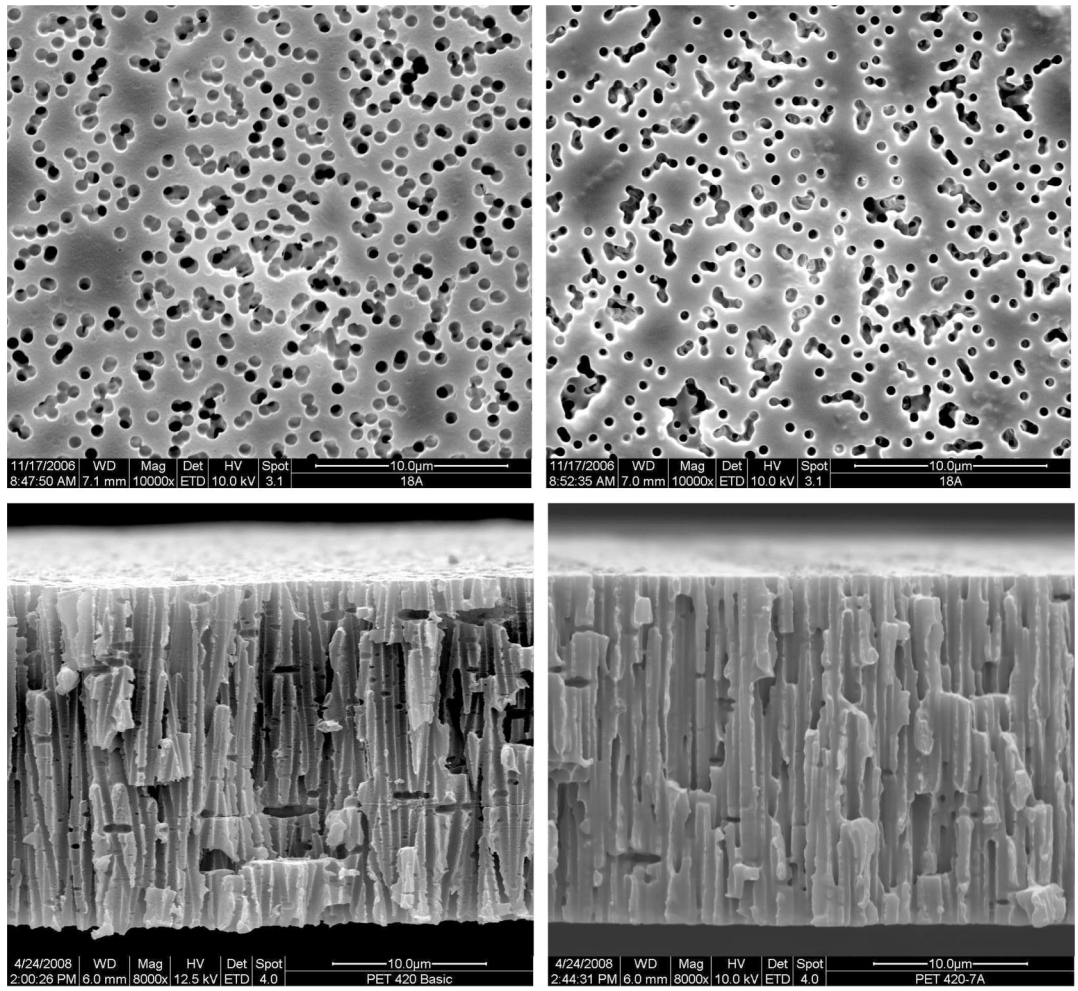

Figure 1. a (left above): Outer surface of a poly(ethylene terephthalate) track-etched membrane (PET400) prefunctionalized with ATRP initiator. b (right above): Outer surface of a PET400 membrane after ATRP grafting of PNIPAAm (DG ~18 μg/cm^2). c (left below): cross-section of a PET400 membrane prefunctionalized with ATRP initiator. d (right below): Cross-section of a PET400 membrane after ATRP grafting of PNIPAAm (DG ~18 μg/cm^2).

track-etching.[35,38,41] Results of our previous work had indicated that the polymer-analogous reactions "oxidative hydrolysis" and subsequent amidation of carboxyl groups with ethanolamine are necessary to immobilize, via esterification of the thus introduced surface hydroxyl groups, the α-bromoisobutyryl ATRP initiator in a high density on the PET surface. In that previous study, however, we had only determined the surface concentrations of carboxyl groups via reversible adsorption of thionin acetate, while the values for the hydroxyl group density on the surface were not known exactly.[37] Bruening et al.[26] had demonstrated that the hydroxyl groups in the side chains of grafted poly(2-hydroxyethyl methacrylate) can be converted nearly quantitatively to carboxyl groups, via a ring opening reaction with succinic anhydride in presence of 4-(*N*′,*N*′-dimethylamino)pyridine. This derivatization should also allow the quantification of hydroxyl on PET using the established staining with thionin acetate (cf. Supporting Information). Results for PET400 are shown in Table 2; similar values were obtained for PET1000 membranes.

As expected, after derivatization with succinic anhydride an increased thionin acetate adsorption was observed after each step of prefunctionalization, except for the final step, the introduction of ATRP initiator. The suitability of the described method is strongly supported by the fact that the amount of dye adsorption was exactly doubled after derivatization of the virgin membranes. By comparing the sum of surface reactive groups between oxidized and prefunctionalized membranes it should be kept in mind that PET swells in contact with DMF,[42] and this may lead to partial detachment of previously introduced groups. As prefunctionalization for ATRP initiator immobilization we selected the derivatization of carboxyl groups with ethanolamine so that the surface density of ATRP initiator was identical to our previous work.[37] The large reduction of hydroxyl group density supports the expectation that a quantitative conversion of surface hydroxyl with α-bromoisobutyryl bromide had been achieved. That the apparent carboxyl density was also largely reduced in this step can be explained by sterical hindrance for dye binding to carboxylic groups on PET by neighbored bulky $COC(CH_3)_2Br$ groups. The resulting initiator surface density of ≤1 groups/nm^2 is in the same range as values for a self-assembled monolayer model system on gold (~3

Table 2. Surface Concentrations of Functional Groups Relative to Specific Surface Area on Poly(ethylene terephthalate) Track-Etched Membranes (PET400) at Different Stages of Pre-Functionalization before ATRP Grafting (for the Method See also Supporting Information)

	surface concentration [groups/nm^2]	
step of synthesis	−COOH	−OH
virgin membrane	0.2	0.2
after oxidative hydrolysis	1.4	0.5
after prefunctionalization with 100% ethanolamine	0.6	0.9
after immobilization of ATRP initiator	0.1	0.1

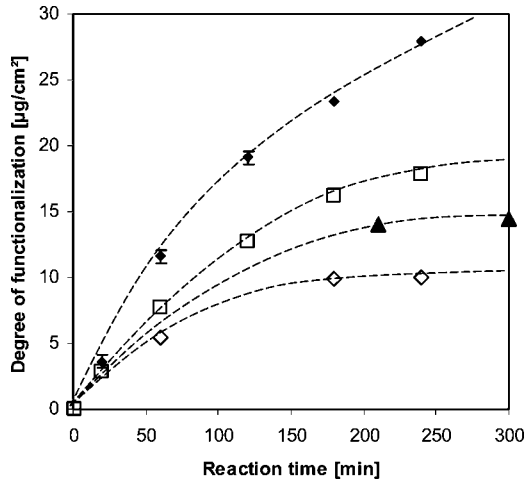

Figure 2. Degree of functionalization (DG), relative to specific surface area, of poly(ethylene terephthalate) track-etched membranes grafted with NIPAAm in DMF as a function of reaction time at ambient temperature. PET1000/♦ = 4.25 mol/L NIPAAm, ▲ = 2 mol/L NIPAAm; PET400/□ = 4.25 mol/L NIPAAm, ◊ = 2 mol/L NIPAAm.

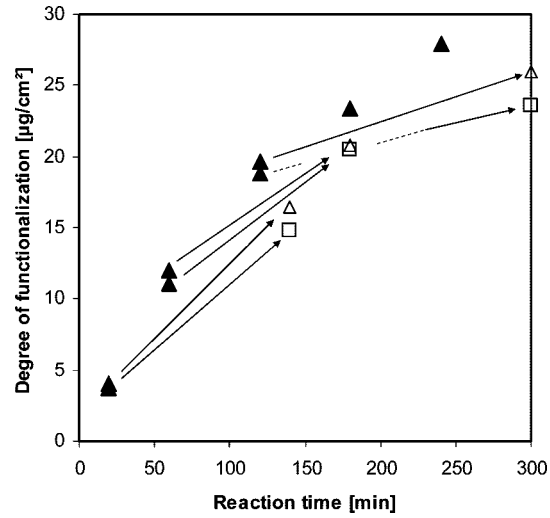

Figure 3. Degree of functionalization (DG), relative to specific surface area, on poly(ethylene terephthalate) track-etched membranes (PET1000) grafted with NIPAAm in DMF as a function of reaction time at ambient temperature: (▲) grafted with 4.25 mol/L NIPAAm in DMF (cf. Figure 2); (□) reinitiated with 2 mol/L NIPAAm in DMF; (Δ) reinitiated with 4.25 mol/L in DMF.

groups/nm^2) used for surface-initiated ATRP,[27,43] and it is far beyond what will be mandatory to achieve grafted polyacrylate-based brushes (cf. ref 12).

Synthesis and Characterization of Grafted Polymer Layers in PET Pores. Our objective was to find a suited reaction system what allows a controlled surface-initiated ATRP of both monomers (the more hydrophilic NIPAAm and the hydrophobic tBA) and a sufficient reaction rate at room temperature. Another important aspect is high reinitiation efficiency after a first grafted block had been quenched, a prerequisite to synthesize in subsequent steps diblock structures. The used solvent should be able to dissolve hydrophilic and hydrophobic monomers and their respective polymers as well as the amphiphilic combinations of both polymers. Therefore, our decision was to use DMF, along with the catalyst system first reported by Masci et al. [34] (cf. above). Also, DMF is a polar medium ensuring the solubility of the fraction of the copper(II) complex which is formed during the preparation of the reaction mixture, and this is also necessary for a controlled ATRP.[44]

PET-*g*-PNIPAAm and PET-*g*-PNIPAAm-*b*-PNIPAAm. When controlled surface-initiated polymerization takes place in porous substrates, two different size-dependent effects could be observed: (i) monomer depletion in the pore volume (for a membrane immersed in an excess of monomer solution only relevant when the chain propagation rate is higher than the monomer diffusion rate, with both rates a function of monomer concentration), and (ii) increasing steric hindrance with layer growth toward the pore interior. The consequence in both cases would be a decrease in grafting rate, and under identical conditions such an effect would occur earlier for smaller pores. Figure 2 shows the influence of pore size and monomer concentration on surface initiated ATRP.

At high NIPAAm concentration in PET1000, ATRP could be performed with good control for up to 4 h. However, the curves for PET400 deviated significantly from the almost linear slope. At the beginning, the membranes were filled with fresh monomer solution; comparison of monomer diffusivity under functionalization conditions with the relatively slow overall grafting rate revealed that monomer depletion in the pore volume should not impose a major limitation. However, the effect of the concave geometry onto increasing probability of termination reactions of active chains can not be ignored: The deviations from linear growth occurred at effective layer thicknesses which were still considerably smaller than the pore radius (less than 100 nm layer thickness for 60 min at 4.25 mol/L compared to pore radius of 380 nm for PET400; cf. below).

In the next series of experiments, selected PET1000 samples, grafted with 4.25 mol/L NIPAAm, were used as macroinitiator for another ATRP to synthesize homo diblock polymers. The NIPAAm concentration in this second step was also varied. Figure 3 shows that all samples increased their DG after the second ATRP. It was possible to reinitiate the sample with a relatively large first block (11 μg/cm^2) with 2 mol/L NIPAAm so effectively that the total DG after another 120 min (20 μg/cm^2) was significantly higher than in case of the one-step series at 2 mol/L time where a plateau of DG had been reached around 12 μg/cm^2 (cf. Figure 2). Similar trends were observed for smaller and larger size of the first block. Obviously, the growth rate of the second block is strongly influenced by the amount of still living chain ends. Nevertheless, it became also clear that each reinitiation leads to a slightly attenuated efficiency as indicated by a consistently lower slope for all second growth reactions when compared with the one-step synthesis at 4.25 mol/L.

Figures 4 and 5 show effective hydrodynamic layer thickness at varied temperature calculated from pure water permeability as a function of the estimated dry layer thickness for all different grafted membranes.

As observed for previous cases where similar PET TEM had been grafted with PNIPAAm via photoinitiation[36] or surface-initiated ATRP in methanol/water,[37] a good correlation of wet layer thickness with dry layer thickness over a wide range and a pronounced change of wet layer thickness with temperature below and above the lower critical solution temperature had been obtained in this study as well. However, quantitative data were markedly different. The ratio of the slopes (wet_{25} vs wet_{45}) obtained for both PET1000 and PET400 was around 1.8 what indicates an equal grafted layer structure in both types of membranes. That both slopes were smaller in PET1000 than in PET400 had also been observed before for photografted membranes;[36] that the value at 45 °C in this study was significantly smaller than 1 can be explained with a surface roughness, in the range of 10s of nanometers, in the PET pores in combination with an especially compact structure of the

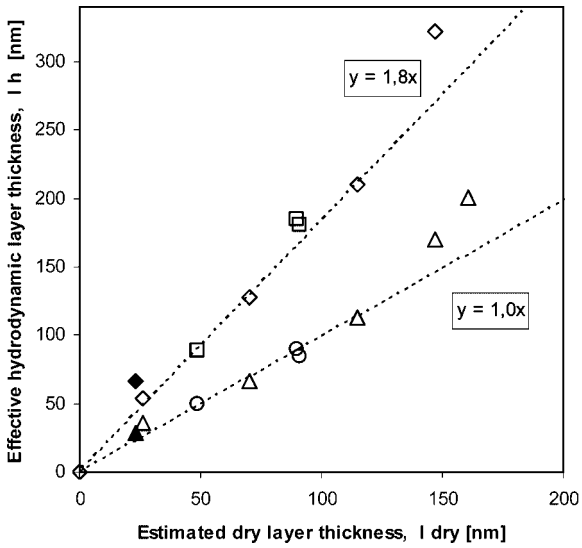

Figure 4. Effective hydrodynamic layer thickness of grafted PNIPAAm in pores of poly(ethylene terephthalate) track-etched membranes (PET400) at 23 and 45 °C, calculated from pure water permeability as a function of the dry layer thickness estimated from degree of functionalization relative to specific surface area and dry polymer density. (Δ,◊) synthesized with 4.25 mol/L NIPAAm; (○,□) synthesized with 2 mol/L NIPAAm; (▲,♦) PET-*g*-PNIPAAm-*b*-PNIPAAm samples.

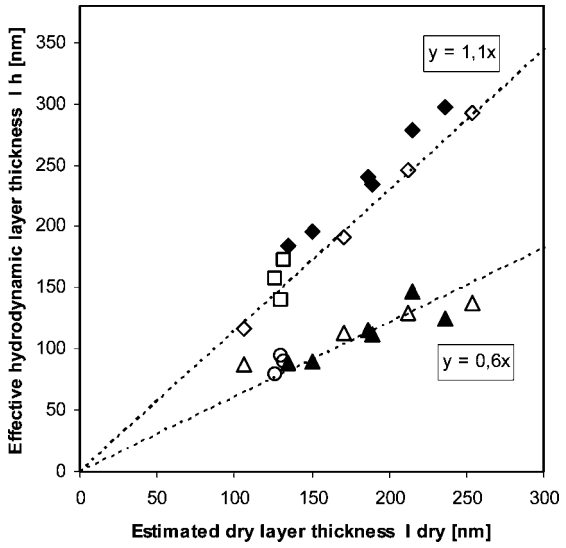

Figure 5. Effective hydrodynamic layer thickness of grafted PNIPAAm in pores of poly(ethylene terephthalate) track-etched membranes (PET400) at 23 and 45 °C, calculated from pure water permeability, as a function of the dry layer thickness estimated from degree of functionalization relative to specific surface area and dry polymer density: (Δ,◊) synthesized with 4.25 mol/L NIPAAm; (○,□) synthesized with 2 mol/L NIPAAm; (▲,♦) PET-*g*-PNIPAAm-*b*-PNIPAAm samples.

grafted layer (cf. below). This observation, however, indicates that the estimation of density of the grafted layer may involve a systematic error (larger for PET1000 than for PET 400).

The temperature switch effects of the membranes synthesized in DMF (with copper(I) chloride/Me_6TREN) were considerably smaller than the data obtained for another ATRP system (methanol/water 7:3 (v:v)/copper(I) bromide/*N*,*N*,*N*′,*N*″,*N*‴-pentamethyl diethylenetriamine) using exactly the same pre-functionalization (ratio wet_{25} vs wet_{45} ~3).[37] The apparent average density of the swollen polymer synthesized in DMF was ~0.55 g/cm^3 (in PET400) and thus much higher than the highest value for synthesis in methanol/water (0.37 g/cm^3), where the chains in the grafted layers were already well in the "brush" regime.[37] This indicates that the achieved grafting densities were even higher, and this can directly be related to the more controlled character of the polymerization: Indeed, almost linear growth could be observed for up to 4 h (cf. Figure 2), while in our earlier study a significant decay of growth rate had been observed already after a few minutes.[37]

Assuming a stretched macromolecule conformation in such "brush" layer and a length per monomer unit of ~0.3 nm, the molar mass of the surface tethered PNIPAAm can be estimated. For instance, for PET1000 with a DG of ~28 μg/cm^2 where 300 nm effective hydrodynamic thickness in swollen state had been measured, the molecular weight would be up to 1×10^5 g/mol. By increasing the ratio between monomer and initiator a larger molecular weight of the polymer can be achieved. For example, Mao et al. polymerized 2-(*N*,*N*-dimethylamino)ethyl methacrylate via ATRP in solution, and for a ratio monomer/initiator/catalyst/ligand of 1800:1:1:1 and 24 h reaction time at 50 °C a molecular weight of ~1.1×10^6 g/mol at a polydispersity of 1.26 had been achieved.[45] In case of a heterogeneous polymerization, the excess of monomer to surface-bound initiator can only be estimated, but it is typically at least in the same range (1000 fold or more). Consequently, the above estimation of average chain length (for 4 h polymerization time at room temperature) seems at least reasonable.

The observed switch effects of the reinitiated homo diblock samples were slightly larger as compared to samples synthesized with only one grafting period. The slightly reduced efficiency of reinitiation discussed above would lead to a lower average grafting density (indicated by a lower apparent average polymer density in swollen state), and it would also cause a larger change of macromolecule's conformation upon transition from swollen to deswollen state.

In addition, we note that the data for PET400 membranes with dry layer thicknesses >150 nm significantly deviate from the linear fit toward larger values. This effect can be interpreted with an influence of the concave pore structure, i.e., the increasing confinement with increasing layer thickness leads to a larger reduction of pore size than what would have been observed for the same grafted layer on planar or convex surface. An analogous effect had been observed and discussed for PET400 membranes grafted with PNIPAAm from methanol/water.[37] However, that this deviation occurs in this work only for dry thicknesses >150 nm and not already for dry thicknesses >80 nm as in ref 37 is well in line with the above discussion, i.e., the higher grafting density and better control achieved with the ATRP system used in this study.

PET-*g*-PtBA, PET-*g*-PtBA-*b*-PtBA and PET-*g*-PAA Obtained via Deprotection. To enable a direct comparison of the results with NIPAAm, experiments for surface-initiated ATRP of tBA have been performed under identical conditions including DMF as solvent (Figure 6). The increase of DG with time was almost linear. However, it was slower than for NIPAAm, and it did not make a difference if 2 or 4.25 mol/L tBA were used. Apparently, limitation by monomer depletion in the pores was not effective for this slower reaction (cf. above). Kizhakkedathu et al. had studied ATRP grafting from latex particle surfaces and found that the more reactive NIPAAm leads to a much lower grafting density (~factor 8) as compared to the less reactive *N*,*N*′-dimethylacrylamide under the same reaction conditions.[46,47] However, in this study tBA is more reactive than NIPAAm (reactivity: acrylates > acryl amides > *N*-substituted acryl amides).[8,10] Therefore, we assume that grafting density of PtBA should be lower than for PNIPAAm. Consequently, the observed slower rate for DG increase (cf. Figure 6) would be caused by the fact that the higher propagation rate can not overcompensate the lower grafting density.

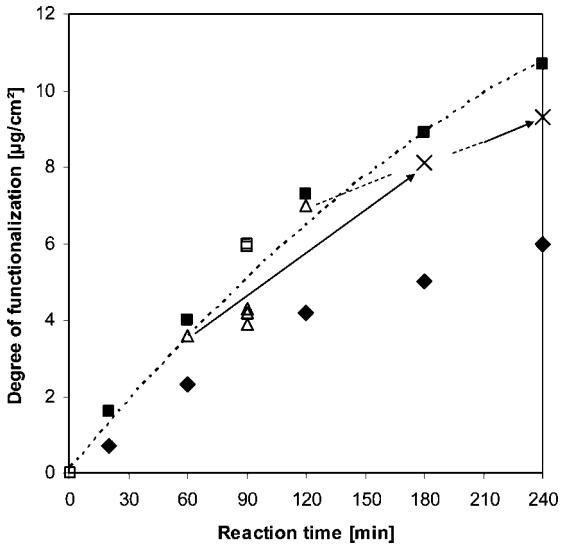

Figure 6. Degree of functionalization (DG), relative to specific surface area, of poly(ethylene terephthalate) track-etched membranes (PET400) as function of reaction time for surface-initiated ATRP at ambient temperature in DMF: (Δ) synthesized with 4.25 mol/L tBA; (■,□) synthesized with 2 mol/L tBA. *X* = PET-*g*-PtBA-*b*-PtBA block samples, obtained after reinitiation with 2 mol/L tBA; (♦) PET-*g*-PAA, obtained via hydrolysis of PET-*g*-PtBA with methansulfonic acid in dichloromethane at ambient temperature (DG corrected for weight loss of PET due to dichloromethane).

In order to investigate the reinitiation using PET-*g*-PtBA macroinitiator membranes, we used samples which were synthesized in the first ATRP using 4.25 mol/L tBA, and the reinitiation for a second ATRP was carried out with 2 mol/L tBA. In general, reinitiated PtBA samples showed a significantly smaller deviation from samples which were polymerized in only one step up to the intended layer thickness than PNIPAAm samples (cf. Figure 3); i.e., the apparent reinitiation efficiency was higher. This difference may be related to the higher reactivity of tBA than NIPAAm, but the lower grafting density and lower effective layer thickness (absolute DG values), both compared to the PNIPAAm experiments (cf. Figure 2), could also have an influence.

Other groups had also reported about the relatively easy reinitiation of acrylates. Tomlinson et al. and Kim et al. had worked on the synthesis of poly(methyl methacrylate) multiblocks on self-assembled monolayers and investigated the efficiency of reinitiation.[44,48] In both studies it had been found that there was no discrepancy if the ATRP was performed with several quench and reinitiation processes or if the ATRP was carried out in one single step. However, the difference to our experiments is that our dry layer thicknesses of PtBA (and PNIPAAm) are 2−3-fold higher. Further, we found for both polymers a point, at which the efficiency of reinitiation decreases clearly.

To determine the DG of the first grafted block the samples were washed, dried and subsequently weighted (cf. above). The polymer layer swelled again when the samples were saturated with the second reaction solution. Macromolecule chains may become entangled during this process, so that the accessibility of active chain ends by monomer may be hindered in the reswollen macroinitiator layer. This may explain why the reinitiation efficiency is decreasing with increasing DG of the first block (cf. Figures 3 and 6). It should be noted that, compared to the results of Kim et al.[44] for a methyl acrylate system in acetonitrile/anisol, our system (copper(I) chloride/Me_6TREN/DMF) leads to a ∼3-fold faster and much more controlled growth of the film from the surface. This confirms that it is always a matter of "system fine tuning" to keep an ATRP "alive" over the required reaction time to reach a desired grafted film thickness.

To obtain stimuli-responsive PAA brushes in the pores of PET TEM, the grafted PtBA had to be selectively deprotected. Many groups reported about quite drastic reaction conditions to "deprotect" PtBA,[49−52] but those conditions would be detrimental for the PET substrate. Therefore, we performed the reaction according to Bruening et al.,[11] under mild conditions with a 1% methanesulfonic acid solution in dichloromethane in just 15 min and obtained quantitative conversion (for results of FT-IR characterization and gravimetric analysis, see Supporting Information).

After hydrolysis, the samples were also characterized via gravimetry. Independent of their DG, all samples (diameter 25 mm) lost (102 ± 18) μg more than the calculated mass loss for complete conversion of PtBA to PAA. This corresponds to ∼0.8% of the membrane samples' average mass. Various control experiments with samples before PtBA grafting revealed that this mass loss is due to the solvent dichloromethane. Apparently, dichloromethane can dissolve short fragments from the PET which had remained in the membrane up to this step. If this correction is considered, the observed ratio DG_{PAA}/DG_{PtBA} is nearly identical to the theoretical value ($M_{w,PAA}/M_{w,PtBA} = 0.562$). This is additional support for having achieved quantitative hydrolysis of grafted PtBA to PAA brushes. That the experimental ratio does not depend on DG may indicate that dissolution of grafted polymer along with the extracted PET fraction is not significant.

An alternative approach to synthesize surface-tethered PAA had been investigated by Husson et al., via ATRP of sodium acrylate at pH 7 in an aqueous copper(I) chloride/Me_6TREN system; the polymerization was controlled, but only a dry PAA thickness of 9 nm could be obtained in 20 h at ambient temperature.[32] In a recent paper, the same group had improved this system via polymerizing the acrylate at pH 10.2 in a concentrated aqueous sodium chloride solution, so that a dry PAA thickness of about 40 nm could be obtained in only 2 h, but the disadvantage was that this ATRP did no proceed in a controlled manner.[27] In our experiments, we obtained via surface-initiated ATRP within 4 h and subsequent hydrolysis a dry PAA layer thickness of 54 nm, and that apparently with good control (cf. Figure 6).

Figure 7 shows the effective hydrodynamic layer thicknesses of the synthesized samples, calculated via permeability measurements at 23 °C with buffers of pH 2 and pH 7.

Similar to previous cases where PET TEM had been grafted with PAA via photoinitiation,[35] an increase of swollen versus dry layer thickness and a pronounced change of wet layer thickness with pH above and below the pK_a of PAA have been obtained in this study as well. The PAA-grafted membranes showed, in comparison with the PNIPAAm-grafted membranes obtained under analogous conditions (cf. Figure 4), a 3−4-fold larger switching effect. A major reason for this difference is the higher equilibrium swelling capability of PAA in buffer at pH 7 in comparison to PNIPAAm in water at 23 °C.[53,54] Another reason might be the lower grafting density of the PAA chains caused by the higher reactivity of tBA, as discussed above.

PET-*g*-PNIPAAm-*b*-PAA and PET-*g*-PAA-*b*-PNIPAAm. For the synthesis of polymer brushes on PET pores which can respond to two different stimuli, consisting of PAA and PNIPAAm blocks, we attempted to graft the monomers tBA and NIPAAm in both sequences by using the conditions for controlled surface-initiated ATRP developed before (cf. above). pH-responsive PAA blocks were obtained by deprotection of grafted PtBA blocks. Table 3 summarizes the reaction conditions for selected successful preparations of such grafted diblock structures.

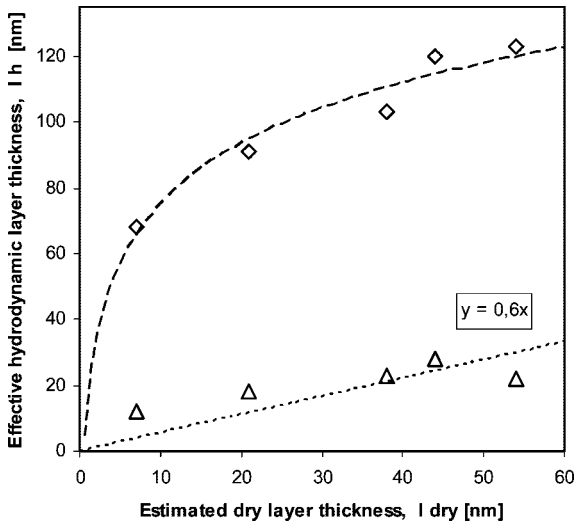

Figure 7. Effective hydrodynamic layer thickness of grafted PAA in pores of poly(ethylene terephthalate) track-etched membranes (PET400), calculated from buffer permeability at 23 °C, as a function of the dry layer thickness estimated from degree of functionalization relative to specific surface area and dry polymer density: (Δ) pH 2 (citrate buffer); (◊) pH 7 (phosphate buffer). All membranes had been synthesized via ATRP with 2 mol/L tBA in DMF and subsequent deprotection (cf. Figure 6).

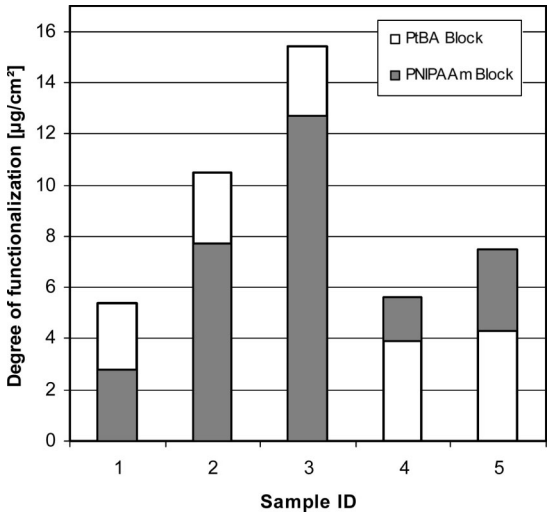

Figure 8. Gravimetric data (degree of functionalization, DG) of the synthesized PET-*g*-PNIPAAm-*b*-PtBA and PET-*g*-PtBA-*b*-PNIPAAm samples; for ATRP conditions see Table 3.

Three different PET-*g*-PNIPAAm membranes prepared with varied reaction time and having the same DG as shown above (cf. Figure 2) were used for a grafting of tBA in a second ATRP step (these macroinitiator samples had been dried and gravimetrically characterized, and their permeability at 23 and 45° had been measured with pure water; cf. Figure 4). The reaction time to synthesize the second block was always 60 min; results are shown in Figure 8 (samples 1−3). In the sequence PET-*g*-PNIPAAm-*b*-PtBA it did obviously not play a role for the DG

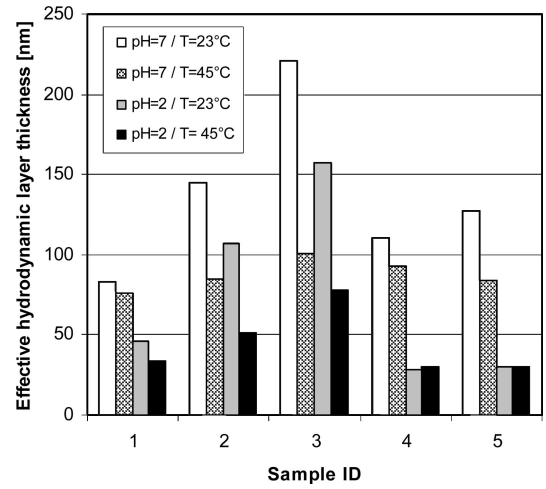

Figure 9. Effective hydrodynamic layer thicknesses of the grafted diblock copolymers in poly(ethylene terephthalate) track-etched membranes (PET400) (cf. Figure 8 and Table 3), calculated from permeability data measured with citrate buffer (pH 2) and phosphate buffer (pH 7) at 23 and 45 °C.

of the grafted PtBA block which size the first PNIPAAm block had, the DG difference was the same ((2.7 ± 0.1) μg/cm^2). If this DG value is compared with the grafting results after the same reaction time for an ATRP-initiator immobilized PET surface (4 μg/cm^2; cf. Figure 6), reinitiation efficiency seems to be ∼75% relative to initiation efficiency. On the other hand, all three membranes had a sufficient amount of active chains leading to same additional amount of grafted polymer. This is further indirect evidence for the lower grafting density which is obtained with tBA compared to NIPAAm. The fact that we found in all three cases, even for the shortest first PNIPAAm block, the same loss (∼25%) with respect to utilization of macroinitiator chain ends, confirms a general rule. Living polymerizations can only be performed with close to 100% reinitiation efficiency, when the synthesis will be started with the more reactive monomer.[8,10,55] To alter this rule, i.e., to increase reinitiation efficiency in the reverse order, ATRP can be carried out using a so-called "halogen exchange".[8,10] On the surface the reaction starts with a tertiary bonded alkyl bromine initiator, but the grafting is carried out using a copper(I) chloride/Me_6TREN system, and after quenching the first block, a chlorine atom will remain at the chain end. This variant had been used successfully throughout this work, but some loss of active chain ends upon starting the second block could not be prevented.

The first experiments toward the inverted sequence (PET-*g*-PtBA-*b*-PNIPAAm) were done using two different PET-*g*-PtBA membranes with DG of 3.6 and 7.0 μg/cm^2. The conditions were 2 mol/L NIPAAm in DMF and 60 min reaction time; however, no change in sample weight was observed. Experiments using PET-*g*-poly(*tert*-butyl methacrylate) membranes with DG of 2.0 μg/cm^2, along with 2 or 4.25 mol/L NIPAAM in DMF for 180 min reaction time were also without any success. In order to check whether the PET-*g*-PtBA membranes had still macroinitiator properties, reinitiation with tBA was performed, and the results were identical with the data already presented in Figure 6.

Table 3. Overview on Reaction Conditions To Synthesize Grafted Diblock Copolymers via Two-Step Surface-Initiated ATRP from the Surface of Poly(ethylene terephthalate) Track-Etched Membranes (PET400; Monomer Concentration Was Always 4.25 mol/L)

sample ID	polymer block I	reaction time I [min]	solvent	polymer block II	reaction time II [min]	solvent (v/v)
1	PNIPAAm	20	DMF	PtBA	60	DMF
2	PNIPAAm	60	DMF	PtBA	60	DMF
3	PNIPAAm	120	DMF	PtBA	60	DMF
4	PtBA	90	DMF	PNIPAAm	240	DMF/2-Bu 1:1
5	PtBA	90	DMF	PNIPAAm	960	DMF/2-Bu 1:1

Scheme 2. Proposed Behavior of Dual-Responsive Block-Copolymer Layers with PAA at Lower Grafting Density as "Inner" Block and PNIPAAm as "Outer" Block (PET-*g*-PAA-b-PNIPAAm): ⋯ = PAA block, — = PNIPAAm Block[a]

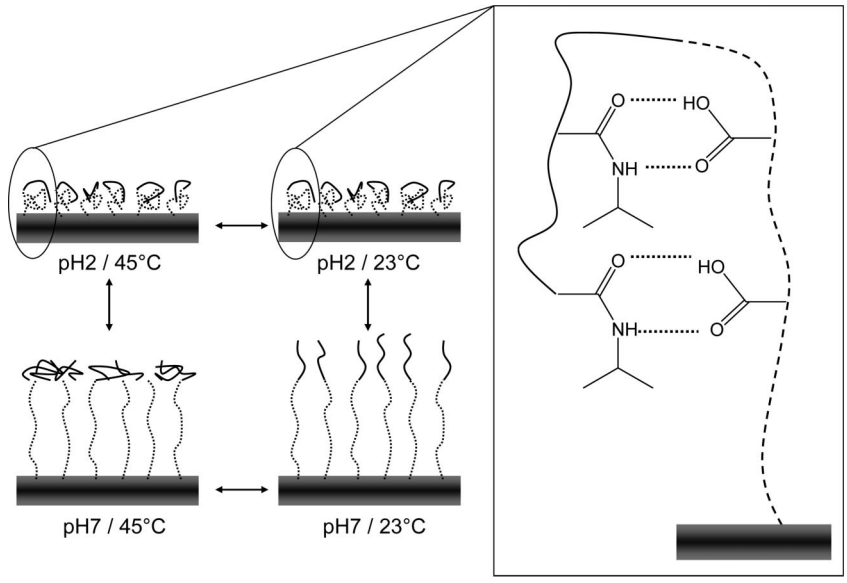

[a] Multiple hydrogen bonding between protonated PAA and PNIPAAm segments will facilitate the back-folding of PNIPAAm segments into the "inner" PAA layer.

Tomlinson et al. had reported that in some cases the optimization of the solvent is the key which permits the synthesis of block copolymer structures containing moieties with quite different properties.[48] For example, surface-initiated ATRP of 2-hydroxyethyl methacrylate from poly(methyl methacrylate) macroinitiators on self-assembly modified gold substrates only succeeded by adding acetone in the solvent mixture whereas the synthesis of poly(methyl methacrylate) multiblocks was possible in methanol/water without adding acetone. Therefore, we also tried to modify the solvent in order to achieve a better solubility of the first PtBA block, and used the work of Li et al.[52] as guide-line: PtBA-*b*-PNIPAAm block copolymers were successfully synthesized in solution with an isopropanol/2-butanone mixture as solvent. With two PET-*g*-PtBA macroinitiator membranes of same DG, ATRP was done using the higher monomer concentration (4.25 mol/L) for 240 and 960 min; the results are shown in Figure 8 (samples 4 and 5).

Significant grafting and increasing DG with reaction time have been observed. Especially, it should be noticed that the polymerization seems to be still "living" after 4 h; DG was approximately doubled between 4 and 16 h. In contrast, long time experiments synthesizing PET-*g*-PNIPAAm from PET400 within up to 21 h revealed that using 4.25 mol NIPAAm the system gets inactive after 4 h. For even lower monomer concentration, the layer stops growing even earlier (cf. Figure 2). The results for grafting NIPAAm on PET-*g*-PtBA may be explained by the already discussed effect that the first PtBA block had been synthesized at lower grafting density than grafting occurs in PET-*g*-PNIPAAm. In addition, the solubility of PtBA in DMF/NIPAAm mixtures seems to be poor, irrespective the addition of 2-butanone. Both influences lead to a lower growth rate of the second PNIPAAm block from PET-*g*-PtBA.

Figure 9 summarizes the effective hydrodynamic layer thicknesses of the blockcopolymer-grafted PET membranes after the deprotection of PtBA to yield PAA blocks, calculated from permeability data measured with citrate (pH 2) and phosphate (pH 7) buffer, respectively, at two different temperatures (23 and 45 °C). When the data for the precursors of membranes #1 to #3 in water (Figure 3) are compared with the data of the block copolymer membranes #1 to #3 (cf. Figure 9), it is obvious that the total layer thickness measured at pH 2 is smaller despite the additional PAA layer. This can be explained by the fact that the PNIPAAm layers are somewhat less swollen in buffer; Geismann et al. had investigated and discussed the underlying salt effects in detail.[36] Both buffers used to adjust pH contain sufficiently high salt concentration to induce this effect.

PET-*g*-PNIPAAm-*b*-PAA membranes #1 to #3 show, as expected for a combination of two stimuli-responsive polymers, four distinctly different pore diameters, controlled by the combination of both different stimuli. The temperature effect is systematically increasing with the DG of the first PNIPAAm block. The pH effect is about the same for all three membranes what is in line with the same added DG of PAA in the outer block. Further the switch effect relative to DG is larger for PAA than for PNIPAAm, and this can related to higher equilibrium swelling capacity of PAA (cf. above) and, presumably, a contribution of lower grafting density of the outer layer (cf. above). Membranes #1 to #3 behave exactly as described in the conceptual cartoon shown in Scheme 1. In case of membrane #1, the "outer" PAA block has a dominating effect because the "inner" PNIPAAm block is relatively short.

PET-*g*-PAA-*b*-PNIPAAm membranes #4 and #5 show only three distinct pore diameters and corresponding effective layer thicknesses as function of the combination of both different stimuli. The pH effect is very pronounced at both temperatures, and this can be related to the significant DG for the first ("inner") block. While the temperature effect at high pH is increasing with the DG of PNIPAAm introduced as second ("outer") block, no temperature response can be seen at low pH where the "inner" PAA layer is deswollen. When considering the lower grafting density of this first PAA block (as discussed above), the PNIPAAm in the "outer" layer is able to fold back into the "inner" layer. Similar to other examples for complexes between PAA and polyacrylamides,[56] multiple hydrogen bonds between protonated PAA and PNIPAAm segments will serve as enthalpic driving force at lower temperature. Increase of temperature above LCST will not change this compact structure of two mixed polymers significantly (Scheme 2). The significantly higher grafting density of the "inner" layer in case of membranes #1 to #3 prohibits backfolding effectively (cf. ref [57]).

The swollen thickness of g-PAA (DG = 2.3 μg/cm^2) at pH 7 was 90 nm (cf. Figure 7); the total thickness grew to

110 or 127 nm, respectively, after second grafting of the less-swelling PNIPAAm (ΔDG: 1.7 and 3.2 $\mu g/cm^2$, respectively). In addition, the significant temperature-induced switching effects observed at pH 7 as function of a relatively small PNIPAAm amount, strongly indicate that these relatively short PNIPAAm chains should be distributed on the chains ends of the first block, i.e., really form an "outer" layer. This would rule out the theoretically possible alternative, that PNIPAAm could be grafted to ATRP initiator sites on the PET, leading to a cografted brush layer of two homo polymers (for examples of such layers cf. ref 2). Even considering our arguments that the grafting density of the PAA layer on PET is lower than for PNIPAAm on PET, we believe that the experimental evidence obtained from the permeability measurements in the cylindrical pores confirms that block copolymer architectures have been achieved for both sequences.

An improved grafting for such structures is still challenging; this and other difficult monomer/polymer combinations are currently being investigated.

Conclusion

A "well tuned" system for surface initiated ATRP allows the controlled functionalization of PET capillary pore membranes with end-on grafted double-responsive block copolymers. The effective layer thickness of the grafted layers could be changed in four steps by up to 200 nm via different combinations of pH (between 2 and 7) and temperature (23 and 45 °C). By this study, the potential of this versatile controlled polymerization technique has been further extended in previously less investigated but very important areas, i.e. the functionalization of technical polymers (instead of metal or ceramic materials) and of concave geometries (instead of planar substrates or particles). Similar to previous work on grafted homo polymers,[3,35−37,58] we have again demonstrated that the PET TEM with their well-defined cylindrical pore morphology are a most versatile tool for the development of grafting conditions and for the detailed characterization of grafted polymer layers. However, such membranes itself could also be developed to new materials, e.g. for controlled (stimulated) release of drugs. Because dry layer thicknesses of up to several hundred nanometers can be reached with good control in relatively short reaction time, the preparation of switchable "valves" in the upper nanometer or even lower micrometer scale should also be possible based on the established conditions. This knowledge will be relevant for the development of new functional ("smart") modules, for instance for "lab-on-a-chip" systems for bio- and medicine technologies.

Supporting Information Available: Text discussing and figure depicting the determination of the pore size distribution, text discussing the analysis of the surface reactive groups, gravimetric analysis, and FT-IR characterization, a scheme showing the derivatization of groups on the surface, and a figure showing the FT-IR difference spectra of two different membranes. This material is available free of charge via the Internet at http://pubs.acs.org.

References and Notes

(1) Kumar, A.; Srivastava, A.; Galaev, L. Y.; Mattiasson, B. *Prog. Polym. Sci.* **2007**, *32*, 1205–1237.
(2) Ionov, L.; Houbenov, N.; Sidorenko, A.; Stamm, M.; Minko, S. *Adv. Funct. Mater.* **2006**, *16*, 1153–1160.
(3) Ulbricht, M. *Polymer* **2006**, *47*, 2217–2262.
(4) Idota, N.; Kikuchi, A.; Kobayashi, J.; Sakai, K.; Okano, T. *Adv. Mater.* **2005**, *17*, 2723–2727.
(5) Eddington, D. T.; Beebe, D. J. *Adv. Drug Deliv. Rev.* **2004**, *56*, 199–210.
(6) Atencia, J.; Beebe, D. J. *Nature* **2005**, *437*, 648–655.
(7) Kato, K.; Uchida, E.; Kang, E. T.; Uyama, Y.; Ikada, Y. *Prog. Polym. Sci.* **2003**, *28*, 209–259.
(8) Matyjaszewski, K.; Xia, J. *Chem. Rev.* **2001**, *101*, 2921–2990.
(9) Edmondson, S.; Osborne, V. L.; Huck, W. T. S. *Chem. Soc. Rev.* **2004**, *33*, 14–22.
(10) Braunecker, W. A.; Matyjaszewski, K. *Prog. Polym. Sci.* **2007**, *32*, 93–146.
(11) Dai, J.; Bao, Z.; Sun, L.; Hong, S. U.; Baker, G. L.; Bruening, M. L. *Langmuir* **2006**, *22*, 4274–4281.
(12) Plunkett, K. N.; Zhu, X.; Moore, J. S.; Leckband, D. E. *Langmuir* **2006**, *22*, 4259–4266.
(13) Matyjaszewski, K.; Dong, H.; Jakubowski, W.; Pietrasik, J.; Kusumo, A. *Langmuir* **2007**, *23*, 4528–4528.
(14) Kim, J. B.; Bruening, M. L.; Baker, G. L. *J. Am. Chem. Soc.* **2000**, *122*, 7616–7617.
(15) Jeyaprakash, J. D.; Samuel, S.; Dhamodharan, R.; Rühe, J. *Macromol. Rapid Commun.* **2002**, *23*, 277–281.
(16) Ma, H.; Wells, M., Jr.; Chilkoti, A. *Adv. Funct. Mater.* **2006**, *16*, 640–648.
(17) Luo, N.; Husson, S. M.; Hirt, D. E.; Schwark, D. W. *J. Appl. Polym. Sci.* **2004**, *92*, 1589–1595.
(18) Liu, D.; Chen, Y.; Zhang, N.; He, X. *J. Appl. Polym. Sci.* **2006**, *101*, 3704–3712.
(19) Liu, Y. L.; Luo, M. T.; Lai, J. Y. *Macromol. Rapid Commun.* **2007**, *28*, 329–333.
(20) Huang, X.; Wirth, M. *J. Anal. Chem.* **1997**, *69*, 4577–4580.
(21) Matyjaszewski, K.; Miller, P. J.; Shukla, N.; Immaraporn, B.; Gelman, A.; Luokala, B. B.; Siclovan, T. M.; Kickelbick, G.; Vallant, T.; Hoffmann, H.; Pakula, T. *Macromolecules* **1999**, *32*, 8716–8724.
(22) Zhai, G.; Kang, E. T.; Neoh, K. G. *Macromolecules* **2004**, *37*, 7240–7249.
(23) Singh, N.; Husson, S. M.; Zdyrko, B.; Luzinov, I. *J. Membr. Sci.* **2005**, *262*, 81–90.
(24) Xu, F. J.; Zhao, J. P.; Kang, E. T.; Neoh, K. G.; Li, J. *Langmuir* **2007**, *23*, 8585–8592.
(25) Yang, Q.; Tain, J.; Hu, M. X.; Xu, Z. K. *Langmuir* **2007**, *23*, 6684–6690.
(26) Sun, L.; Dai, J.; Baker, G. L.; Bruening, M. L. *Chem. Mater.* **2006**, *18*, 4033–4039.
(27) Singh, N.; Wang, J.; Ulbricht, M.; Wickramasinghe, S. R.; Husson, S. M. *J. Membr. Sci.* **2008**, *309*, 64–72.
(28) Shibayama, M.; Tanaka, T. *Adv. Polym. Sci.* **1993**, *109*, 1–62.
(29) Chen, G.; Hoffman, A. S. *Nature* **1995**, *373*, 49–52.
(30) Peng, T.; Cheng, Y. L. *Polymer* **2001**, *42*, 2091–2100.
(31) Xia, F.; Feng, L.; Wang, S.; Sun, T.; Song, W.; Jiang, W.; Jiang, L. *Adv. Mater.* **2006**, *18*, 432–436.
(32) Lindqvist, J.; Nystroem, D.; Oestmark, E.; Antoni, P.; Carlmark, A.; Johansson, M.; Hult, A.; Malmstroem, E. *Biomacromolecules* **2008**, *9*, 2139–2145.
(33) Sankhe, A. Y.; Husson, S. M.; Kilbey, S. M. *Macromolecules* **2006**, *39*, 1376–1383.
(34) Masci, G.; Giacomelli, L.; Crescenzi, V. *Macromol. Rapid Commun.* **2004**, *25*, 559–564.
(35) Geismann, C.; Ulbricht, M. *Macromol. Chem. Phys.* **2005**, *206*, 268–281.
(36) Geismann, C.; Yaroshchuk, A.; Ulbricht, M. *Langmuir* **2007**, *23*, 76–83.
(37) Friebe, A.; Ulbricht, M. *Langmuir* **2007**, *23*, 10316–10322.
(38) Alem, H.; Duwez, A. S.; Lussis, P.; Lipnik, P.; Jonas, A. M.; Champagne, S. D. *J. Membr. Sci.* **2008**, *308*, 75–86.
(39) Ciampolini, M.; Nardi, N. *Inorg. Chem.* **1966**, *5*, 41–44.
(40) Matyjaszewski, K.; Tsarevsky, N. V.; Braunecker, W. A.; Dong, H.; Huang, J.; Jakubowski, W.; Kwak, Y.; Nicolay, R.; Tang, W.; Yoon, J. A. *Macromolecules* **2007**, *40*, 7795–7806.
(41) Marchand-Bryneart, J.; Deldime, M.; Dupont, I.; Dewez, J. L.; Schneider, Y. L. *J. Colloid Interface Sci.* **1995**, *173*, 236–244.
(42) Gozdz, A. S.; Weigmann, H. D. *Textile Research J.* **1984**, *54*, 9–17.
(43) Liu, Y.; Klep, V.; Zdyrko, B.; Luzinov, I. *Langmuir* **2004**, *20*, 6710–6718.
(44) Kim, J. B.; Huang, W.; Bruening, M. L.; Baker, G. L. *Macromolecules* **2002**, *35*, 5410–5416.
(45) Mao, B. W.; Gan, L. H.; Gan, Y. Y. *Polymer* **2006**, *47*, 3017–3020.
(46) Kizhakkedathu, J. N.; Norris-Jones, R.; Brooks, D. E. *Macromolecules* **2004**, *37*, 734–743.
(47) Kizhakkedathu, J. N.; Kumar, K. R.; Goodman, D.; Brooks, D. E. *Polymer* **2004**, *45*, 7471–7489.
(48) Tomlinson, M. R.; Efimenko, K.; Genzer, J. *Macromolecules* **2006**, *39*, 9049–9056.
(49) Cai, Y.; Hartenstein, M.; Müller, A. H. E. *Macromolecules* **2004**, *37*, 7484–7490.
(50) Colombani, O.; Ruppel, M.; Schubert, F.; Zettl, H.; Pergushov, D. V.; Müller, A. H. E. *Macromolecules* **2007**, *40*, 4338–4350.
(51) Rathfon, J. M.; Tew, G. N. *Polymer* **2008**, *49*, 1761–1769.

(52) Li, G.; Shi, L.; An, Y.; Zhang, W.; Ma, R. *Polymer* **2006**, *47*, 4581–4587.
(53) Philippova, O. E.; Hourdet, D.; Audebert, R.; Khokhlov, A. R. *Macromolecules* **1997**, *30*, 8278–8285.
(54) Diez-Pena, E.; Quijada, I.; Barrales-Rienda, J. M. *Macromolecules* **2002**, *35*, 8882–8888.
(55) Debuigne, A.; Warnant, J.; Jerome, R.; Voets, I.; de Keizer, A.; Cohen Stuart, M. A.; Detrembleur, C. *Macromolecules* **2008**, *41*, 2353–2360.
(56) Bergbreiter, D. E.; Case, B. L.; Liu, Y. S.; Caraway, J. W. *Macromolecules* **1998**, *31*, 6053–6062.
(57) Li, B.; Xu, L.; Chen, T.; Sun, P.; Jin, Q.; Ding, D.; Wang, X.; Xue, G.; Shi, A. C. *Macromolecules* **2007**, *40*, 5776–5786.
(58) He, D. M.; Ulbricht, M. *Macromol. Chem. Phys.* **2007**, *208*, 1582–1591.

MA802185D